Vision Research 105 (2014) 199–203

Contents lists available at ScienceDirect

Vision Research

journal homepage: www.elsevier.com/locate/visres

# Coding depth perception from image defocus

Hans Supèr [a,b,c,*], August Romeo [a]

[a] Dept. of Basic Psychology, Faculty of Psychology, University of Barcelona (UB), Spain
[b] Institute for Brain, Cognition and Behavior (IR3C), Spain
[c] Catalan Institution for Research and Advanced Studies (ICREA), Spain

ARTICLE INFO

*Article history:*
Received 4 July 2014
Received in revised form 3 October 2014
Available online 31 October 2014

*Keywords:*
Depth from defocus
Chromatic aberration
Spiking model

ABSTRACT

As a result of the spider experiments in Nagata et al. (2012), it was hypothesized that the depth perception mechanisms of these animals should be based on how much images are defocused. In the present paper, assuming that relative chromatic aberrations or blur radii values are known, we develop a formulation relating the values of these cues to the actual depth distance. Taking into account the form of the resulting signals, we propose the use of latency coding from a spiking neuron obeying Izhikevich's 'simple model'. If spider jumps can be viewed as approximately parabolic, some estimates allow for a sensory-motor relation between the time to the first spike and the magnitude of the initial velocity of the jump.


## 1. Introduction

The visual system of spiders includes layers which receive defocused images containing depth information. A remarkable behavioural experiment reported in Nagata et al. (2012) has shown that depth perception is affected by light wavelength through the variable amount of defocus related to the chromatic aberration. This observation has resulted in a specific mechanism proposed by the authors of that work. Although it is not immediate to establish direct relations between this model and the responses in humans or other vertebrates, there are a number of aspects more or less evidently connected with its working.

The question of ocular control determined by chromatic defocus has been object of study in humans and guinea pigs in Kotulak, Morse, and Billock (1995) and Qian et al. (2013) and Refs. therein. Accommodative gain in humans depends on the chromatic bandwith of the stimulus under dynamic conditions (the present work offers a simplified approach in which bandwith issues are not considered, but they are undoubtedly present in the real world).

In vision systems with two sensor classes, each with different wavelength sensitivity, chromatic aberrations can be exploited. For such a category, which includes the human eye with their L and S cones, chromatic aberrations provide a signed cue to defocus (Fincham, 1951; Flitcroft, 1990). This is possible because the aberration introduces a sign-dependent tendency for one sensor class to have greater amplitudes than the other. At the same time, monochromatic aberrations can provide an odd-error cue to focus direction (Wilson, Decker, & Roorda, 2002), as blur shape may lead to the detection of differences in the appearance of the point spread function (PSF) between myopic and hyperopic defocus. For humans, adaptations to blur changes are important because adjustments may play a role in tuning the match between cortical responses and the spatial structure of images (Webster, Georgeson, & Webster, 2002).

Perception of depth from defocus (DFD) is a well established concept, and the idea of using changes in focus settings has been in circulation for a long time. Computationally oriented outlooks are offered by e.g. (Chaudhuri & Rajagopalan, 1999) or (Schechner & Kiryati, 2000), while recent psychological or biological considerations are better illustrated by papers like Mather and Smith (2000), Held, Cooper and Banks (2012), and Read (2012), and bibliography therein. Regarded as a source of defocus estimation, blur seemed to be just a complementary cue, the pre-eminent one being stereoscopic disparity. However, blur is not so weak as previously guessed. While disparity is more precise near fixation blur is more precise away from the focusing plane (Held, Cooper, & Banks, 2012; Read, 2012).

In the calculation of DFD, blur differences between images are employed as a cue for distance estimation. Accurate blur evaluation from natural scenes is in general a difficult problem which shall not be addressed in the present work. Instead, we will assume that the values of the relevant variables have already been extracted from the visual input. Even such a simple method as measuring the 'edge bleeding' length is applicable only in cases where the image is binary and contained in a single plane perpendicular to the line of gaze. Procedures based on transfer functions usually require some amount of frequency-based reasoning. In fact, real data always depend on the present space frequencies, and that

* Corresponding author.

http://dx.doi.org/10.1016/j.visres.2014.10.022
0042-6989/

sort of limitation would also constrain the information from the spider eye. After the classical papers (Pentland, 1987; Subbarao, 1988), many techniques have been devised for the calculation of blur parameters, tackling major issues such as the presence of noise (Chaudhuri & Rajagopalan, 1999), space invariance (Chaudhuri & Rajagopalan, 1999; Jin & Favaro, 2002), the geometric model (Favaro & Soatto, 2005) or the nature of the employed filters (Watanabe & Nayar, 1998; Burge & Geisler, 2011).

A study of responses to perturbations in Schechner and Kiryati (2000) showed that for the case of two-dimensional DFD using a circularly symmetric lens-aperture the *aperture problem* does not appear. From that viewpoint, DFD allows for more robust estimations (however, note that the comparison involved stereo systems made of ideal cameras, not biological pupils).

In the present paper we wish to make an explicit formulation of the idea in Nagata et al. (2012). Supposing that the problem of measuring the chromatic aberration or the blur radii from the images themselves has already been solved at some previous stage, we concentrate on the question of setting up some neural coding for the obtained magnitudes, and suggest the use of spike latency. The proposal is illustrated by a numerical simulation of a spiking neuron hypothetically doing this job.

## 2. Methods

Efficient visual systems should enable animals to obtain food and avoid predators. Jumping spiders try to jump accurately enough to catch their preys. They are equipped with two pairs of principal eyes (PEs) and anterior lateral eyes (ALEs). Even if ALEs are occluded jumps can be precise, showing that PEs suffice for absoulte depth perception. The remarkable point is that PEs do not have overlapping fields, thus ruling out stereo effects. Moreover, these eyes have no focal adjustment mechanism, and no moves capable of generating motion parallax have been observed either. Thus, the only remaining explanation lies in the use of blur differences from the different wavelength sensitive parts of the PE retinas (Nagata et al., 2012 and Refs. therein).

A basic way of modelling the function of these PEs is to consider a lens with two focal lengths depending on the wavelength values. Like in Nagata et al. (2012), the starting point is the thin lens equation written in the form

$$\frac{1}{d}+\frac{1}{v}=\frac{1}{F} \tag{1}$$

where $d$ is the object distance, $v$ the image distance and $F$ the focal length. Note that $d>0$ for objects in front of the lens and $v>0$ for images behind the lens. In these conditions, $d$ is al so called 'depth'. The authors of Nagata et al. (2012) study the case of equal image distances $v$ and different perceived depths $d, d'$, caused by the use of different focal lengths, say $F_g, F_r$ with $F_g<F_r$ ('g' for green, 'r' for red). Taking the two equalities and deleting one from the other it is immediate to arrive at

$$d'=\frac{d}{1+df}=\frac{1}{f}\left(1-\frac{1}{1+df}\right),\quad f\equiv\frac{1}{F_g}-\frac{1}{F_r}, \tag{2}$$

which is Eq. (1) in Nagata et al. (2012). The meaning of the present magnitudes is $d'$ = estimated distance, $d$ = true distance.

For this type of lens, the general law relating the absolute values of object and image sizes $R_o, R$, focal length $F$ and object distance $d$ reads

$$R=R_o\,\frac{F}{d-F} \tag{3}$$

In the studied situations, $d>F$.

### 2.1. Aberration method

Different focal values $F$ give rise to different image sizes $R$. Let $R_g, R_r$ indicate the image sizes $R$ of (3) for $F=F_g$ and for $F=F_r$ respectively. The difference $R_r-R_g$ amounts to the lateral or transverse chromatic aberration. We call $\mathcal{C}$ the ratio between this chromatic aberration and one of the two sizes, i.e.

$$\mathcal{C}=\frac{|R_r-R_g|}{R_r}=\frac{d}{d-F_g}\,F_g f. \tag{4}$$

Thus, $\mathcal{C}>0$ for $d>F_g$. From this equation it is straightforward to find the true distance $d$ as a function of $\mathcal{C}$

$$d=\frac{F_g}{1-\frac{\mathcal{C}_\infty}{\mathcal{C}}}\equiv d(\mathcal{C}),\quad \mathcal{C}_\infty\equiv F_g f. \tag{5}$$

Next, we can consider what happens when 'g' and 'r' are interchanged in Eq. (4), i.e., the reference is 'r' instead of 'g', while the $f$ value is kept unchanged. Thus, instead of (4), we are left with

$$\mathcal{C}'=\frac{|R_r-R_g|}{R_g}=\frac{d}{d-F_r}\,F_r f, \tag{6}$$

where we have made use again of (3). At this point, evaluating the $d(\mathcal{C})$ function of Eq. (5) with argument $\mathcal{C}'$, we obtain

$$d'=d(\mathcal{C}')=\frac{F_g}{1-\frac{\mathcal{C}_\infty}{\mathcal{C}'}}. \tag{7}$$

One may care to check that Eqs. (4)–(7) indeed lead to the relation between $d, d'$ already established by Eq. (2).

For this mechanism to work it is necessary to find the relative aberration $\mathcal{C}$ from two image planes by examining the regions where green is distinct and where red is distinct. When the figure is a circle centred at the origin it is possible to obtain $\mathcal{C}=1-R_g/R_r=1-\sqrt{A_g/A_r}$, where $A_g, A_r$ indicate the figure areas in image space for the green-distinct and red-distinct parts (this is an ideal set-up, rather infrequent in the world of real images; the general problem of extracting distance cues is a question which we are here sidestepping). Although simple, the 'lateral chromatic aberration' method requires simultaneous inputs from two planes.

### 2.2. Blur method

In each of the two considered image planes one colour shows a distinct outline and the other a blurred one. Following e.g. Chaudhuri and Rajagopalan (1999) or Pentland (1987), or studying the similar triangles in Fig. 3A of (Nagata et al., 2012), it is easy to reason that the blur radius $b$ amounts to

$$b=\rho\,\frac{|\Delta v|}{v}, \tag{8}$$

where $\rho$ is the lens aperture radius, $v$ denotes the distance from the image plane (focus plane) to the lens, and $\Delta v$ indicates the separation between that plane and the employed sensor plane. From Eqs. (1) and (2), setting equal $d$ and different $F, v$ values for the two cases of $F_r, v_r$ and of $F_g, v_g$, we arrive at $\Delta v=v_r-v_g=v_r v_g f$. Taking into account the colours of the distinct and blurred parts in every case, the radii for the red and green blurs are

$$b_{r,g}=\rho\, v_{r,g} f \tag{9}$$

By combining these relations and (1) again, we obtain two possible forms for the $d$ distance in terms of the blur radii, which are

$$d=\frac{F_r}{1-\frac{F_r f\rho}{b_r}} \tag{10}$$

$$=\frac{F_g}{1-\frac{F_g f\rho}{b_g}}=\frac{F_g}{1-\frac{b_\infty}{b_g}},\quad b_\infty\equiv F_g f\rho. \tag{11}$$

The physical meaning of $b_\infty$ is the green blur radius for $d$ tending to infinity. It may be viewed as the special value of a free parameter - say a sort of 'weight'- to be learnt. Of course, mathematically speaking it is enough to make just one measurement for determining a single parameter, but that could also be the result of some 'learning' procedure, e.g., a minimization of an error function of the type $\varepsilon = (d - d_{\text{expected}})^2$. Assuming that the other parameters are somehow known, object distances may be estimated as a function of the observed blur radius in the considered image plane (and, unlike method 1, one plane suffices). If the animal usually makes estimations from (11), it has somehow learnt the value of the $F_g f\rho$ product. After changing the light type it should apply (10), but keeps using (11) with $b_r$ instead of $b_g$, thus evaluating

$$\frac{F_g}{1-\frac{F_g f\rho}{b_r}} = d' \tag{12}$$

One may check that the $d$ and $d'$ of formulas (10)–(12) satisfy the relation $d' - d = -fdd'$, equivalent to (2), which was the law explaining the results of Nagata et al. (2012).

The ratio between then two blur radii is

$$\frac{b_g}{b_r} = \frac{F_g}{F_r} \quad \frac{d-F_r}{d-F_g} = 1 - \frac{b_g}{\rho}. \tag{13}$$

Note that Eq. (5) as a function of the transverse aberration and Eq. (11) in terms of the blur radius are formally equal. Therefore, any idea about parameter learning can be carried over from one scheme to the other.

### 2.3. Latency coding

The first idea that comes to one's mind is to apply firing rate coding using inputs proportional to the $d$ distance obtained through rule (5) or (11). However, inputs involving functions of the type $f(x) \propto \frac{1}{1-1/x}$ do not seem to be very usual in neural modelling. In addition, for spiking models, rate coding requires long integration times, so that differences in spike numbers can be well appreciated. On the contrary, latency coding only needs the time to the first elicited spike, and looks more advantageous. Most cortical neurons fire spikes with a delay depending on the strength on the received input. For inputs relatively weak, but above threshold, that delay, also called spike latency, can be quite noticeable. Regularly spiking cells in the cortex of mammalians can have latencies of the order of tens of ms. Such delays offer a spike-timing mechanism for encoding the intensity of the input. The benefits of latency coding for another task, namely, coding the spatial structure of flashed images, were discussed in Gollisch and Meister (2008).

For the Izhikevich neuron model Izhikevich (2003, 2004, 2007) in the 'small-$a$ approximation' (Romeo & Supèr, 2014) —which amounts to keeping the quadratic integrate-and-fire level—, the membrane potential of the cell evolves in time according to

$$V(t) = V_m + \sqrt{\bar{I}}\tan\left(\frac{\alpha\sqrt{\bar{I}}}{C}t + \varphi_0\right),$$
$$\varphi_0 = \arctan\left(\frac{V_0 - V_m}{\sqrt{\bar{I}}}\right), \tag{14}$$

where $V_0 = V(0)$ and

$$\bar{I} = \frac{I - I_m - u_0}{\alpha}, \quad I_m = \alpha V_m^2 - \gamma, \quad V_m = -\frac{\beta}{2\alpha}. \tag{15}$$

$\alpha, \beta, \gamma$ are constants of this model, $I$ is the input current, $C$ (not $\mathcal{C}$) indicates the membrane capacitance, and $u_0$ stands for the initial value of the recovery variable $u$. Consider the time to the first spike, say $t = t_1$. Setting $V(t_1) = V_p$ ('peak' potential) implies $t_1 = \frac{C}{\alpha\sqrt{\bar{I}}}\left[\arctan\left(\frac{V_p - V_m}{\sqrt{\bar{I}}}\right) - \varphi_0\right]$. For simplicity we adopt the initial condition $V_0 = V_m$, which leads to $\varphi_0 = 0$. Further, admitting input values of such a scale that $\frac{V_p - V_m}{\sqrt{\bar{I}}} \gg 1$, we apply $\arctan x = \frac{\pi}{2} + \mathcal{O}\left(\frac{1}{x}\right)$ for $x \gg 1$, which takes us to

$$t_1 \simeq \frac{\pi C}{2\alpha\sqrt{\bar{I}}} = \frac{\pi C}{2\sqrt{\alpha(I - I_0)}}, \quad I_0 \equiv I_m + u_0. \tag{16}$$

Next, the question of the relation between neural input and defocus 'hypothetic measurements' has to be addressed. We shall assume that some preprocessing mechanism is sending signals which supply the measured size of either the relative lateral aberration or the blur radius, i.e., $\mathcal{C}$ or $b_g$ is already available. If so, any of them can be used to produce an input $I$ of the form

$$I - I_0 = \kappa \cdot \left\{ \begin{array}{l} \left(\frac{\mathcal{C}}{\mathcal{C}_\infty} - 1\right) \\ \left(\frac{b_g}{b_\infty} - 1\right) \end{array} \right\} = \kappa \frac{F_g}{d - F_g}, \tag{17}$$

where $\kappa$ is some constant with dimensions of current, $\mathcal{C}, \mathcal{C}_\infty$ are the variables of Eqs. (4) and (5), and $b_g, b_\infty$ the magnitudes in (11). The quotients $\kappa/\mathcal{C}_\infty$ or $\kappa/b_\infty$ can be envisaged as 'gain' parameters, while $\kappa$ itself is a contribution to the $I$ bias term. The existence of these two possibilities rests on the analogy between (5) and (11), which leads to the second equality of (17) in both cases. For any of them the input is just linear in the relevant variable ($\mathcal{C}$ or $b_g$). Combination of (16) and (17) yields the approximate spike latency as a function of the distance

$$t_{1g} \simeq \frac{\pi C}{2}\sqrt{\frac{d - F_g}{\alpha\kappa F_g}}. \tag{18}$$

The added 'g' subscript indicates that $t_1$ has been found from $F = F_g$. Hence, $d$ can be 'read out' from $t_{1g}$ by means of $\frac{d}{F_g} = 1 + \frac{4\alpha\kappa}{\pi^2 C^2} t_{1g}^2$. Actually, when the second term on the r.h.s. dominates it is enough to keep

$$d \simeq F_g \frac{4\alpha\kappa}{\pi^2 C^2} t_{1g}^2. \tag{19}$$

This approximation will be good for $d \gg F_g$ with a sufficiently large $\kappa$ value.

From (16)–(19), we can derive the relation between latency $t_{1g}$ and radius $b_g$ for green blur, i.e., $t_{1g} \simeq \frac{\pi C}{2}\sqrt{\frac{b_\infty}{\alpha\kappa b_g}}$. As a result, when taking $b_r$ instead of $b_g$ the latency changes by the approximate rule

$$t_{1r} \simeq \sqrt{\frac{b_g}{b_r}}\, t_{1g} = t_{1g}\sqrt{1 - \frac{b_g}{\rho}}, \tag{20}$$

where (13) has been applied. Neglecting $\mathcal{O}\left((b_g/\rho)^2\right)$, we obtain the latency difference $t_{1g} - t_{1r} \simeq \frac{t_{1g} b_g}{2\rho}$, which exhibits to what extent $t_{1r}$ is shorter than $t_{1g}$.

Dropping the colour subscript from $t_1$, and indicating the resolution in spike times by $\Delta t_1$, the associated error in distance resolution $\Delta d$ obeys the approximate law

$$\Delta d = \mathcal{A}\, t_1\, \Delta t_1, \quad \mathcal{A} \equiv \frac{8 F_g \alpha\kappa}{\pi^2 C^2}. \tag{21}$$

## 3. Results and discussion

### 3.1. Simulation

A comparison between simulated and approximate $t_1$ values is shown in Fig. 1. The employed focal values were $F_g = 1$ mm,

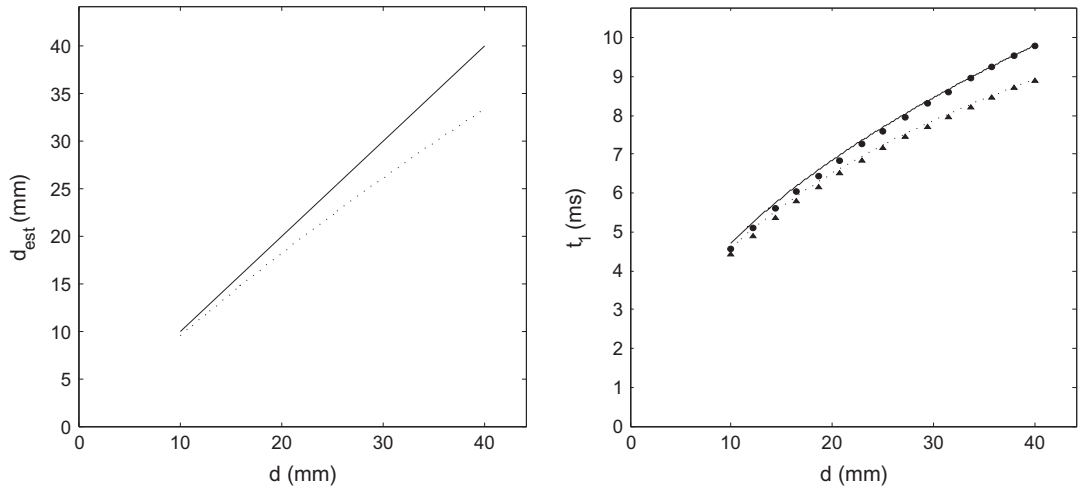


**Fig. 1.** Results for $F_g \simeq 1$ mm and $f \simeq 5 \cdot 10^{-3}\,(\text{mm})^{-1}$, roughly similar to the set-up of Nagata et al. (2012). Left: theoretically obtained distances $d$ from green blur (solid line) and underestimated $d'$ based on red blur (dotted line). Right: time to first elicited spike $t_1$ as a function of the real distance $d$, when the received inputs involve the values of $F_g$ and $F_r$. Symbols denote the outcome of numerically simulating an RS Izhikevich neuron with inputs given by Eq. (17) and the parameter values quoted in the text (circles for green blur, triangles for red blur) while lines indicate the analytical approximations (solid for green blur, dotted for red blur).

$f = 5 \cdot 10^{-3}\,(\text{mm})^{-1}$, and the neuron parameters $C = 1$ μF, $\alpha = 0.04$ μA/(mV)$^2$, $\beta = 5$ μA/mV, $\gamma = 140$ μA (which are the coefficients in Izhikevich's model for currents measured in μA), $\kappa = (1/0.04)$ μA [so that $\alpha\kappa = 1\,(\mu\text{A})^2/(\text{mV})^2$], and the neuron parameters of the regularly spiking (RS) type given in Izhikevich (2003): $a = 0.02\,(\text{ms})^{-1}, b = 0.2$ μA/mV, $c = -65$ mV, $d = 8$ μA. The Euler method was applied with a time step $\Delta t = 5 \cdot 10^{-2}$ ms. As can be seen, in the studied set-up, which is similar to the scenario of Nagata et al. (2012), the agreement between numerical simulation and theoretical approximation is quite good.

Introducing the employed parameters in (21), and imagining a 'readout' resolution of $\Delta t_1 = 1$ ms, the distance error $\Delta d$ of Eq. (21) for $t_1 = 5$ ms amounts to 4 mm.

### 3.2. Motor response

So far we have shown a model based on simple assumptions attributed to the environmental needs of spiders, in particular, to their quest for preys. After gathering experimental knowledge about their visual system, a chromatic scheme was formulated. Taking advantage of that model we have been able to establish an approximate relationship between target distance and spike latency. At the present stage, an interesting speculation would be to wonder whether the 'readout' (19) can be related to any variable which determines the motor response aimed at catching the prey. In order to give an answer we have to make some sort of assumption about the trajectory of the jump made by the animal. These jumps may be described by motions in a constant gravitational field. Being accurate, spiders cannot really be regarded as point-like objects, as they may offer a sizable ratio of surface area to mass density. As air drag can in general play a role, one could think of including a braking force $\vec{F}_{\text{braking}} = -\mathfrak{b}\vec{v}$, where $\mathfrak{b}$ is a constant which depends on the medium and on the geometrical properties of the body, and $\vec{v}$ indicates the velocity vector.

Following the textbook (Symon, 1971), we see that for small values of $\mathfrak{b}$,

$$d = \frac{v_0^2}{g}\sin(2\phi)\left[1 - \frac{4}{3}\frac{\mathfrak{b}v_0}{mg}\sin(\phi) + \ldots\right], \tag{22}$$

where $v_0$ is the magnitude of the initial velocity, $\phi$ the jumping angle relative to the horizontal —or 'shoot angle'—, $g$ the acceleration of gravity, and $m$ the mass of the animal. The unwritten terms are contributions of higher order when $\mathfrak{b}$ is small. If we content ourselves with rough estimations, a situation of small drag may be approximated by just the $\mathfrak{b} = 0$ contribution, which amounts to the well-known parabolic result

$$d = \frac{v_0^2}{g}\sin(2\phi). \tag{23}$$

Comparing (19) and (23) we eliminate $d$ and arrive at

$$t_1 \simeq \frac{\pi C}{2}\sqrt{\frac{\sin(2\phi)}{\alpha\kappa F_g g}}\,v_0. \tag{24}$$

We have thus found a 'motor' meaning for the 'latency' $t_1$: for a given angle, $t_1$ is proportional to $v_0$, the magnitude of the initial velocity for the jump. Taking $\sin(2\phi) \simeq 1$, $t_1$ of the order of 10 ms, and the quoted parameter values, $v_0$ is of the order of 1 m/s, which corresponds to a jump of around 4 cm. In principle, a perturbative approach in $\mathfrak{b}$ from (22) might supply successive corrections for small nonzero values of this constant.

In contrast, when the braking effects are important $\mathfrak{b}$ is large and, according to the discussion in Symon (1971), $d$ can sometimes be approximated by

$$d \simeq \frac{mv_0}{\mathfrak{b}}\cos(\phi). \tag{25}$$

Then, the same comparison leads to

$$t_1 \simeq \frac{\pi C}{2}\sqrt{\frac{m}{\mathfrak{b}}\frac{\cos(\phi)}{\alpha\kappa F_g g}}\,v_0. \tag{26}$$

Thus, in this situation, instead of a linear relation of the form $t_1 \propto v_0$, the main contribution to $t_1$ is of the type $t_1 \propto v_0^{1/2}$. Further, unlike in (24), the value of $t_1$ depends now on $m/\mathfrak{b}$.

## 4. Conclusions

Manifest formulations of the concepts contained in Nagata et al. (2012), concerning the effects of light wavelength on depth perception, have been provided. Granting that the extent of the chromatic aberration or the blur radius can be computed from the perceived images themselves, we have derived expressions relating their values to the actual target distance, reproducing the length underestimation remarked in Nagata et al. (2012). In view of the form of

the input signals, we suggest using a type of latency coding where the distance is an increasing function of the time to the first spike. A numerical simulation, based on a widely accepted neural model, indicates that it can offer good performance in terms of resolution. Assuming that spider jumps can be described by shoot trajectories, approximate estimates give grounds for establishing a sensory-motor relation, between the time to the first elicited spike and the magnitude of the shoot velocity. In the case of negligible aero-dynamical effects they are linearly related, but in situations with very large braking forces that time is proportional to the square root of the magnitude of the shoot velocity.

While in the presented model inputs are based on wavelength selection (like in the experiment of Nagata et al. (2012)), a natural environment would actually provide similar information based on distance. Unlike our simplified set-up, real tasks satisfying the environmental needs of the animal would call for an efficient read-out and processing of all the existing distance cues from the visual input, which undoubtedly pose a much more complex challenge.

## References


Burge, J., & Geisler, W. S. (2011). Optimal defocus estimation in individual natural images. *Proceedings of the National Academy of Sciences of the United States of America, 108*, 16849–16854.

Chaudhuri, S., & Rajagopalan, A. N. (1999). *Depth from defocus, a real aperture imaging approach*. Springer.

Favaro, P., & Soatto, S. (2005). A geometric approach to shape from defocus. *IEEE Transactions on Pattern Analysis and Machine Intelligence, 27*, 406–417.

Fincham, E. F. (1951). The accommodation reflex and its stimulus. *The British Journal of Ophthalmology, 35*, 381–393.

Flitcroft, D. I. (1990). A neural and computational model for the chromatic control of accommodation. *Visual Neuroscience, 5*, 547–555.

Gollisch, T., & Meister, M. (2008). Rapid neural coding in the retina with relative spike latencies. *Science, 319*, 1108–1111.

Held, R. T., Cooper, E. A., & Banks, M. S. (2012). Blur and disparity are complementary cues to depth. *Current Biology, 22*, 426–431.

Izhikevich, E. M. (2003). Simple model of spiking neurons. *IEEE Transactions on Neural Networks, 14*, 1569–1572.

Izhikevich, E. M. (2004). Which model to use for cortical spiking neurons? *IEEE Transactions on Neural Networks, 15*, 1063–1070.

Izhikevich, E. M. (2007). *Dynamical systems in neuroscience: The geometry of excitability and bursting*. Cambridge, MA: MIT Press.

Jin, H., & Favaro, P. (2002). A variational approach to shape from defocus. In *European conference on computer vision. Lecture notes in computer science* (vol. 2351, pp. 18–30). Springer.

Kotulak, J. C., Morse, S. E., & Billock, V. A. (1995). Red-green opponent channel mediation of control in human ocular accommodation. *Journal of Physiology, 482*, 697–703.

Mather, G., & Smith, D. R. R. (2000). Depth cue integration: Stereopsis and image blur. *Vision Research, 40*, 3501–3506.

Nagata, T., Koyanagi, M., Tsukamoto, H., Saeki, S., Isono, K., Shichida, Y., et al. (2012). Depth perception from image defocus in a jumping spider. *Science, 335*, 469–471.

Pentland, A. P. (1987). A new sense for depth of field. *IEEE Transactions on Pattern Analysis and Machine Intelligence, 9*, 523–531.

Qian, Y-F., Dai, J-H., Liu, R., Chen, M-J., Zhou, X-T., & Chu, R-Y (2013). Effects of the chromatic defocus caused by interchange of two monochromatic lights on refraction and ocular dimension in guinea pigs. *PLoS ONE, 8*, e63229.

Read, J. C. A. (2012). Visual perception: Understanding visual cues to depth. *Current Biology, 22*, R163–R165.

Romeo, A., & Supèr, H. (2014). Approximations to the time evolution of an Izhikevich neuron. *International Journal of Modern Physics C, 25*, 1450052.

Schechner, Y. Y., & Kiryati, N. (2000). Depth from defocus vs. stereo: How different really are they? *International Journal of Computer Vision, 39*, 141–162.

Subbarao, M. (1988). Parallel depth recovery by changing camera parameters. *International Conference of Computer Vision*, 149–155.

Symon, K. R. (1971). *Mechanics* (3rd ed.). Massachusetts: Addison-Wesley.

Watanabe, M., & Nayar, S. K. (1998). Rational filters for passive depth from defocus. *International Journal of Computer Vision, 27*, 203–225.

Webster, M. A., Georgeson, M. A., & Webster, S. M. (2002). Neural adjustments to image blur. *Nature Neuroscience, 5*, 839–840.

Wilson, B. J., Decker, K. E., & Roorda, A. (2002). Monochromatic aberrations provide an odd-error cue to focus direction. *Journal of the Optical Society of America, 19*, 833–839.